



RESEARCH ARTICLE

Classification of mammograms by breast density

N. Sasirekha¹, Jayakumar Karuppaiah², Yuvaraja Thangavel³, K G Parthiban⁴

Abstract

The risk of getting breast cancer is directly affected by the type of breast tissue predominant in the individual. The aim is to investigate histogram-based image attributes in order to separate mammographic images by degree of breast density using the clustering technique. 75 mammographic images from the MIAS database were used, 25 of them belonging to each of the three classes: fatty, fatty-glandular and dense. After the selection of attributes, it obtained a 96% success rate in classifying the mammograms within the three classes when the attribute's mean gray levels and the highest peak intensity of the histogram were used simultaneously in the clustering technique.

Keywords: Clustering, breast density, attribute extraction.

Introduction

Breast cancer is the most common neoplasm in women and one of the highest causes of death among females. The implementation of screening programs has contributed to a significant reduction in the mortality rate due to early diagnosis, with digital mammography currently being the mainstay of the screening program for breast cancer (Radiology ACO (2003)).

Breast density, by itself, represents a risk factor for the development of breast tumors and decreases the sensitivity of mammography (Cuzick *et al.*, (2004), McCormack *et al.*, (2006), Petroudi *et al.*, (2003)). The relative risk is estimated to be 4 to 6 times greater when comparing women with a percentage of fibroglandular tissue greater than 75% with

women with less than 25%. This constitutes a limitation to mammography due to the masking effect, which results from overlapping and, consequently, from the lack of contrast between the lesions and the fibroglandular tissue. For this reason, the greater the breast density, the lower the sensitivity and specificity of mammography. Additionally, increased breast density is associated, at the time of diagnosis, with increased size of lesions and a worse prognosis (Boyd *et al.*, (2005), Ramya *et al.* (2015), Vanitha *et al.* 2022).

This can be classified, according to the Breast Image Reporting and Data System (BIRADS) classification of the ACR - American College of Radiology, by visual estimation of the percentage of fibroglandular tissue compared to the percentage of adipose tissue, into four categories – category A, B, C and D (Petroudi *et al.*, (2003), Oliver *et al.*, (2005), Bosch *et al.*, (2006), Muštra *et al.*, (2012)), with women with dense breast tissue often associated with categories C and D, while women with less dense breast tissue are included in categories A and B of this classification.

The growing technique of tomosynthesis has shown very good results with regard to increased sensitivity for the detection and characterization of lesions. Studies show that this imaging method is particularly useful in young women with denser breasts due to its ability to nullify the effect of tissue overlap. Other authors refer that the combination of tomosynthesis and mammography may contribute to the evolution of screening programs in favor of reducing the rate of false positives in this population Arivazhagan *et al.*, (2003), Haralick *et al.*, (1973), Renno *et al.*, (1998)).

This work aims to investigate image attributes, based on a histogram that separates mammographic images by degree of breast density, through a clustering technique.

¹Department of Electronics and Communication Engineering, Sona College of Technology, Salem, Tamil Nadu, India.

²Department of Biomedical Engineering, KIT-Kalaignarkarananidhi Institute of Technology, Coimbatore, Tamil Nadu, India.

³Department of Electronics and Communication Engineering, Kongunadu College of Engineering and Technology, Trichy, Tamil Nadu, India.

⁴Department of Electronics and Communication Engineering, Dhaanish Ahmed Institute of Technology, Coimbatore, Tamil Nadu, India.

*Corresponding Author: Author, Affiliation, E-Mail:

How to cite this article: Sasirekha, N., Karuppaiah, J., Thangavel, Y., Parthiban, K.G. (2023). Classification of mammograms by breast density. *The Scientific Temper*, 14(3): 811-815.

Doi: 10.58414/SCIENTIFICTEMPER.2023.14.3.38

Source of support: Nil

Conflict of interest: None.

Literature Review

Conant *et al.*, 2019 determined whether screening tests performed with DBT are associated with a better prognosis. Screening with DBT is associated with the detection of smaller lesions and the early detection of invasive tumors, as well as a decrease in the recall rate, when compared to screening with DM.

Alsheik *et al.*, 2019 compared the results associated with breast cancer screening with the use of DM alone versus the combined method. Decreased recall rate in women undergoing screening with DBT.

Rose *et al.*, 2018 evaluated the diagnostic performance of the combined method in screening in comparison with DM alone. Decreased recall rate and increased lesion detection rate with the joint method.

Rosso *et al.*, 2015 investigated which factors affect fraction of false positives. FFP is mainly affected by breast density.

Starikov *et al.*, 2016 determined which modality – DM or DBT, are the most suitable for screening, according to breast density. The combination of DM with DBT contributed to a decrease in the recall rate and an increase in the injury detection rate.

Honig *et al.*, 2019 identified the factors that give rise to false negatives in screening for DM. Decreased recall rate with the use of DBT. The authors previously defend the performance of DBT with DM for comparison.

McCarthy *et al.*, 2014 reported the impact of implementing DBT as a screening technique in an entire clinical population. DBT is associated with a reduction in the recall rate and an increase in the lesion detection rate, both for women with high breast density and for women with lower density.

Destounis *et al.* 2014 compared the results between patients who underwent screening with only DM versus those who underwent screening with the combined method. Reduction of recall rate with the combination of DM and DBT techniques.

Conant *et al.*, 2016 verified whether DBT is associated with an improvement in results from screening. When compared to DM, there is an increased lesion detection rate, specificity and decreased recall rate using DBT.

Margolies *et al.*, 2014 studied the factors that predict the management of the diagnostic process with the use of DBT. Decreased recall rate, false positive rate and increased lesion detection rate, with the combination of DM and DBT techniques, mainly in women with high breast density.

Haas *et al.*, (2013) compared lesion detection rates during DM screening versus the combined method. Decreased recall rate and increased detection rate with the combination of the two techniques, DM and DBT.

This systematic review intends to discuss the results of the literature with regard to the integration of tomosynthesis in screening programs for the evaluation of women with

high breast density, that is, with heterogeneously and extremely dense breast tissue, associated with categories C and D according to the ACR BIRADS classification, respectively. The clinical indicators considered were: recall rate or recall rate - recall rate (percentage of individuals asked to return to the service for repeat or additional tests after a doubtful finding in the initial test), fraction of false positives (FFP) and rate injury detection.

Materials and Methods

The images collected in the Mini-MIAS database (Liberatore *et al.*, (2017)) are reported in three classes, and likewise, this work will make a separation within these three classes according to the database reports: fatty (G), fatty-glandular (GG) and dense (D).

Thus, the three classes of the problem will be: Class 1: fatty (BI-RADSTM Pattern 1), Class 2: fatty-glandular (BI-RADSTM Pattern 2-3) and Class 3: dense (BI-RADSTM Pattern 4).

The images will be separated from the extraction and selection of histogram-based attributes that best separate the images between these three classes, and then a clustering technique will be implemented allowing to grouping each image according to its corresponding class.

Twenty five images of each pattern were used, thus totaling 75 mammographic images, all previously reported according to the density pattern. The images, eight bits per pixel, have a size of 1024 x 1024 and were all obtained on the same equipment.

The images collected are mammograms under a mediolateral oblique view that presented information in texts and labels in addition to the pectoral muscle. It is then noted the need for segmentation, done manually in this work, transforming all this unnecessary information into the background of the image (black-gray level). Figure 1 presents an image before and after the segmentation process.

Note that both the pectoral muscle and the label in the upper right corner shown in Figure 1(a) were removed and transformed into the background, thus disregarding the attribute calculations.

After the segmentation process, the images in RGB pattern were all converted to images in gray levels. With that, it was noticed that some regions considered as background did not present gray level equal to zero (black), but close to this value. Thus, before processing, it was necessary to reduce 10 gray levels of each pixel from all images and only values greater than three were considered in the calculations.

In this case, the range of gray levels considered for the calculation of the histogram and extraction of intensity attributes is from 4 to 245, thus considering only the pixels that are part of the breast and disregarding the background. Nine histogram-based attributes were extracted, cited and explained below:

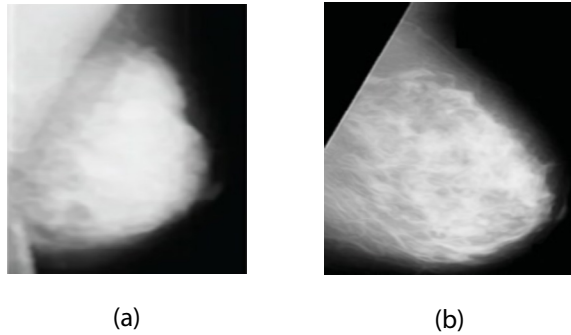


Figure 1: (a) Mammogram collected from the image bank. (b) Image after segmentation

- Average gray levels: corresponds to the sum of the intensity values of each pixel divided by the total number of pixels represented in the histogram;
- Intensity value of the highest histogram peak (mode): intensity value that occurs most in the histogram;
- Highest histogram intensity: highest pixel intensity value found in the histogram;
- Lowest histogram intensity: lowest pixel intensity value found in the histogram;
- Difference from mean to highest value: highest intensity value subtracted from average gray levels;
- Difference from mean to lowest value: average of gray levels subtracted from the lowest intensity value;
- Percentage of highest intensity in relation to maximum intensity: highest pixel intensity value obtained divided by 245 and multiplied by 100 to obtain the percentage;
- Number of pixels greater than the histogram peak: number of pixels with intensity values greater than the histogram peak value;
- No. of pixels in the ROI: highest histogram intensity subtracted from lowest histogram intensity.

Each image obtained a value for each of the attributes. Subsequently, a simple arithmetic average of the attributes was made, in addition to the calculation of the standard deviation for each class, allowing the results to be compared between them. The entire image processing step was performed using the MatLab computational simulator.

After the processing step and having the results of each attribute for each class, the step of selection and classification of attributes, using the same computational simulator. The objective here is to select or which attributes best differentiate the images within each class.

The selection was made based on the normal distribution (Gaussian). Mean and standard deviation parameters entirely describe this method. Knowing these values makes it possible to determine any probability in a normal distribution. The smaller the overlapping of the Gaussian curves of the classes, the more significant the attribute must be, in terms of separability. The classification starts with knowing which attribute best separates the classes.

The clustering technique used was K-means, which aims to partition 'n' observations among 'K' clusters, where each observation belongs to the cluster closest to its mean.

Observations and Discussion

Table 1 below presents the mean values obtained from the 25 images of each class for each of the attributes. These values correspond to the simple arithmetic mean of the values of each class. Before the attribute selection process, not much can be said just by analyzing the results. However, it is noted that some attributes have different values for each class, as is the case with the attributes: 1) Mean gray levels, 2) Largest histogram peak and 3) Difference of mean to smallest value.

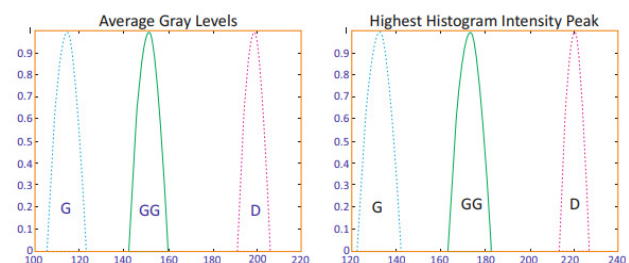
After building the normal distributions of all attributes, it was found that only two attributes, Average gray levels and the highest histogram peak, showed complete separation between classes, as shown in Figure 2.

The highest histogram peak attribute also showed the fact that the dense class, predominantly made of fibroglandular tissue, presented lighter levels, obtaining values closer to 245.

The other attributes had curves overlapping when the normal distribution was drawn, making it impossible to separate the images between classes. Although some

Table 1: Average attribute values for each class

Attribute	Fatty class	Fatty-glandular class	Dense class
1	114.6	151.3	198.4
2	131.8	172.3	219.1
3	210.2	223.8	228.6
4	6.6	6.1	5.9
5	95.6	72.5	30.2
6	108	145.2	192.5
7	85.79	91.34	93.30
8	512.18	735.47	232.86
9	203.6	217.7	222.7



Attributes (1) and (2) proved that there is a difference in the intensity of gray levels between the classes. Visually, the fat class presents darker gray levels because it is predominantly composed of adipose tissue, and this was confirmed with the values obtained by the average gray levels attribute.

Figure 2: Normal distributions for the average gray levels attribute (1) and highest histogram intensity peak (2)

Table 2: Classifier hit percentage for each analyzed attribute

Attribute	Percentage of correct classification (%)
Average gray levels	94.66
Biggest histogram peak	92
Both simultaneously	96

attributes have different mean values, what caused a bad separation was the high standard deviation value of these attributes.

After the correct selection of attributes, the K-Means clustering method was implemented on the two attributes and the classification results are shown in Table 2.

Table 2 shows that when the clustering technique used only the Average gray levels attribute, the classifier's accuracy was 92%. This indicates that of the 75 images, 71 were correctly classified within their class. As for the other attribute, the percentage of correctness was 92%, with six classification errors.

When using both attributes simultaneously, the highest success rate was obtained, 96%, where only three images were classified in classes different from those in which they actually belonged.

Conclusion

The intrinsic subjectivity of the process of classifying mammograms by density pattern in reports is an increasingly difficult process and subject to results with a high degree of confusion.

It is possible to automate this task with acceptable error rates through clustering techniques, as long as the attribute extraction is adequate to the image characteristics that involve the problem. In this case, the pixel intensity and its variation is directly related to the breast density pattern.

It was shown in this work that 97.33% of the mammograms were correctly grouped within their breast density pattern class using histogram attributes. It was clear that when more than one attribute is used simultaneously in the technique, the grouping becomes better, increasing the accuracy of the method. The next stages of the work consist of the implementation of an automatic image segmentation technique, in addition to new tests using a larger number of images.

Acknowledgment

We are thankful to the management for conducting this collaborative study.

References

- Alsheik NH, Dabbous F, Pohlman SK, Troeger KM, Gliklich RE, Donadio GM, *et al.* (2019). Comparison of Resource Utilization and Clinical Outcomes Following Screening with Digital Breast Tomosynthesis Versus Digital Mammography: Findings From a Learning Health System. *Acad Radiol.* v. 26, n. 5, pp. 597–605.
- Arivazhagan S, Ganesan L (2003) Texture classification using wavelet transform. *Pattern Recogn Lett.* v. 24, n. 15, pp. 3-1521
- Bosch A, Muoz X, Oliver A *et al.* (2006) Modeling and Classifying Breast Tissue Density in Mammograms. In: *Comput Vision Pattern Recogn, 2006 IEEE Computer Society Conference on.* pp. 1552-1558.
- Boyd NF, Rommens JM, Vogt K *et al.* (2005) Mammographic breast density as an intermediate phenotype for breast cancer. *The Lan Onco.* v. 6, pp. 798- 808.
- Conant E, Beaber E, Sprague B, Herschorn S, Weaver D, Onega T, *et al.* (2016). Breast cancer screening using tomosynthesis in combination with digital mammography compared to digital mammography alone: a cohort study within the PROSPR consortium. *Breast Cancer Res Treat.* v.156, n. 1, pp. 109.
- Conant EF, Barlow WE, Herschorn SD, Weaver DL, Beaber EF, Tosteson ANA, *et al.* (2019). Association of Digital Breast Tomosynthesis vs Digital Mammography With Cancer Detection and Recall Rates by Age and Breast Density. *JAMA Oncol.* v.5, n. 5, pp. 635–42.
- Cuzick J, Warwick J, Pinney E *et al.* (2004) Tamoxifen and breast density in women at increased risk of breast cancer. *J Natl Cancer I.* v. 96, pp. 621-628.
- Destounis S, Arieno A, Morgan R. (2014). Initial Experience with Combination Digital Breast Tomosynthesis Plus Full Field Digital Mammography or Full Field Digital Mammography Alone in the Screening Environment. *J Clin Imaging Sci.* v. 4, n. 1, pp. 1–6. Available from: <http://10.0.16.7/2156-7514.127838>
- Haas BM, Kalra V, Geisel J, Raghu M, Durand M, Philpotts LE. (2013). Comparison of tomosynthesis plus digital mammography and digital mammography alone for breast cancer screening. *Radiology.* v. 269, n. 3, pp. 694– 700.
- Haralick RM, Shanmugam K, Dinstein IH (1973) Textural features for image classification. in: *IEEE Transactions on Systems, Man, and Cybernetics* (Volume: SMC-3, Issue: 6, November 1973) Page(s): 610 - 621
- Honig EL, Mullen LA, Amir T, Alvin MD, Jones MK, Ambinder EB, *et al.* (2019). Factors Impacting False Positive Recall in Screening Mammography. *Acad Radiol.* v. 26, n. 11, pp. 1505–12.
- Liberatore M, Cucchi JM, Fighiera M, Binet A, Missana MC, Brunner P, Mourou MY, Iannesi A. Interest of systematic tomosynthesis (3D mammography) with synthetic 2D mammography in breast cancer screening. *Horm Mol Biol Clin Investig.* 2017 Dec 16;32(2):j/hmbci.2017.32.issue-2/hmbci-2017-0024/hmbci-2017-0024.xml. doi: 10.1515/hmbci-2017-0024.
- Margolies L, Cohen A, Sonnenblick E, Mandeli J, Schmidt PH, Szabo J, *et al.* (2014). Digital Breast Tomosynthesis Changes Management in Patients Seen at a Tertiary Care Breast Center. *ISRN Otolaryngol.* 2014 Jan;1.
- McCarthy AM, Kontos D, Synnestvedt M, Tan KS, Heitjan DF, Schnall M, *et al.* (2014). Screening Outcomes Following Implementation of Digital Breast Tomosynthesis in a General-Population Screening Program. *JNCI J Natl Cancer Inst.* v. 106, n. 11, pp. 1.
- Mccormack VA, Dos Santos Silva I (2006) Breast density and parenchymal patterns as markers of breast cancer risk: a meta-analysis. *Cancer Epidem Biomar : a publication of the American Association for Cancer Research, cosponsored by the American Society of Preventive Oncology.* v. 15, pp. 1159-1169.

- Muštra M, Grgić M, Delač K (2012) Breast Density Classification Using Multiple Feature Selection. *Automatika: a magazine for automation, measurement, electronics, computing and communications*. v. 53, pp. 362-372.
- Oliver A, Freixenet J, Zwiggelaar R (2005) Automatic classification of breast density. In: *Image Processing, 2005. ICIP 2005. IEEE International Conference on*. IEEE, pp. II-1258-1261.
- Petroudi S, Kadir T, Brady M (2003) Automatic classification of mammographic parenchymal patterns: A statistical approach. In: *Engineering in Medicine and Biology Society, 2003. Proceedings of the 25th Annual International Conference of the IEEE*. IEEE, pp. 798-801.
- Radiology ACO (2003) *Breast imaging reporting and data system, breast imaging atlas*. Reston, USA.
- Rafferty EA, Durand MA, Conant EF, Copit DS, Friedewald SM, Plecha DM, *et al.* (2016). Breast Cancer Screening Using Tomosynthesis and Digital Mammography in Dense and Nondense Breasts. *JAMA*. v. 315, n. 16, pp. 1784–6.
- Renno CD, Freitas CDC, Sant'anna SJS (1998) A system for region image classification based on textural measures. *European Space Agency- Publications-Esa SP*. v. 434, pp. 159-164.
- Rose SL, Shisler JL. (2018). Tomosynthesis Impact on Breast Cancer Screening in Patients Younger Than 50 Years Old. *AJR Am J Roentgenol*. v. 210, n. 6, pp. 1401–4.
- Rosso A, Lang K, Petersson IF, Zackrisson S. (2015). Factors affecting recall rate and false positive fraction in breast cancer screening with breast tomosynthesis - A statistical approach. *Breast*. v. 24, n. 5, pp. 680–6.
- Starikov A, Drotman M, Hentel K, Katzen J, Min RJ, Arleo EK. (2016). 2D mammography, digital breast tomosynthesis, and ultrasound: which should be used for the different breast densities in breast cancer screening? *Clin Imaging*. v. 40. n. 1, pp. 68–71.
- van der Waal, D., Verbeek, A.L.M. & Broeders, M.J.M. Breast density and breast cancer-specific survival by detection mode. *BMC Cancer* 18, 386 (2018). <https://doi.org/10.1186/s12885-018-4316-7>
- L Ramya, N Sasirekha, (2015). A robust segmentation algorithm using morphological operators for detection of tumor in MRI, 2015 International Conference on Innovations in Information, Embedded and Communication Systems (ICIIECS).
- L Vanitha, K Jayamani, N Sasirekha, G Sajiv, (2022). Detection and Classification of Breast Cancer from Microscopic Biopsy Images using Modified Neural Network, 2022 International Conference on Automation, Computing and Renewable Systems